Industrial Engineering Journal
ISSN: 0970-2555
Volume : 53, Issue 12, No.3, December : 2024

ELECTROCHEMICAL SYSTEM ANALYSIS FROM IMPEDANCE DATA TO REINFORCEMENT THERMO MECHANICALLY TREATED (TMT) REBAR

Anjani Kumar Singh, Faculty, Dept. of Mechanical Engineering YBN University, Ranchi-834010, India. anjani232@gmail.com
Shashikant Rajpal, Faculty, Govt. Engineering College, Munger -811201, India

Abstract: The objective of the present investigation is to evaluate the performance of reinforcement thermomechanically treated (TMT) rebars in concrete pore solution with or without mixing with 3.5% NaCl. From potentiodynamic results it is clearly indicated that corrosion of steel (sample-T-SPS) is more in comparison to steel (sample S-SPS) in simulated concrete pore solution and simulated concrete pore solution with addition of 3.5% NaCl.
Keywords: TMT, OCP, NaCl, electrode

I. Introduction

Corrosion of steel rebar in concrete is a major issue in the construction industries. The first article was published in 1900s to address the corrosion of steel rebar embedded in concrete and U.S. Bureau of Standard in 1913 established that the small addition of chloride ion in concrete significantly enhances the corrosion of steel rebar [1]. The corrosion of steel rebar resulted in the premature collapse of concrete structures especially located near the marine or coastal areas [2]. A substantial increase in uses of de-icing salt took place during the last four decades. Due availability of huge amount of salt in concrete structures caused severe corrosion of embedded steel rebar. In 1993 Federal Highway Administration (FHWA) reported that for maintenance of concrete structure from corrosion, the cost of it would be $212 billion, with the cost of annual maintenance being $67 billion through 2011 [3].

II. Experimental Methods

Test materials

The reinforcement thermo mechanically treated (TMT) rebars were cut into different sizes for studies. The chemical compositions of steel rebars were studied by optical emission spectroscopy (Bruker, Germany). Steel rebars were cut by CNC Wire EDM machine, model no. EX 40, India into different sizes for studies. Different types of steel rebars were used to electrochemical tests. As received steel rebars from two different producing companies were cut and pickled in 10 v/v % HCl, thoroughly washed with distilled water, dried and degreased with acetone. The steel rebars used in electrochemical cell were cut in cross section, abraded with different grade of emery paper starting from 100 to 1200 grits followed by cloth polishing, Metco, India with 5 μm alumina paste.

Composition of the concrete pore solutions used

Two different types of solutions were prepared and simulate the concrete pore solution in laboratory scale. Firstly, a solution of sodium hydroxide (NaOH) = 8.33g/L + potassium hydroxide (KOH) = 3.36g/L + calcium oxide (CaO) = 2.0 g/L was used to emulate the fresh concrete pore solution. For the preparation of second solution an amount of 35g/L NaCl was mixed in the prepared simulated concrete pore solution for achieving the aggressiveness of the electrolyte. The solution was kept 24 hours under Microyn magnetic stirrer, model no.SH-2 and then filtered on Wattman paper of No.15 grade. The insoluble CaO was removed from solution [4, 5].

Table 1: Chemical compositions of reinforced steels used in the this study

Wt. % of alloying elements											
Steels	C	Mn	Si	S	P	Ni	As	Cu	Cr	Sn	Fe
S	0.264	0.79	0.19	0.003	0.03	0.02	0.016	0.017	0.051	0.014	Balance
T	0.238	0.73	0.17	0.002	0.01	0.04	0.006	0.003	0.010	0.001	Balance

Industrial Engineering Journal
ISSN: 0970-2555
Volume : 53, Issue 12, No.3, December : 2024

Electrochemical measurements

Electrochemical tests were carried out in SPS solution containing with or without 35g/L NaCl using the standard 3-electrode corrosion cell containing the saturated calomel electrode (SCE) as reference electrode, counter electrode (graphite) and working electrode (the sample). All electrodes were immersed in a suitable glass vessel containing 600 ml of the electrolyte. The anodic and cathodic polarization data were obtained after 1 hr of working electrode immersion at ambient temperature (23± 2°C) in the media. Subsequently, the polarization curves for both steel were scanned from potential -250 mV to 1500 mV**,** from OCP with a scan rate of 100 mV min^{-1}. Corrosion rates were calculated for steel immersed in aqueous solutions using the following equation:-

$$CR = k \times \frac{Icorr}{\rho \times A} \times Ew$$

Where, k is the corrosion rate constant, Icorr is the corrosion current (□A), EW is the equivalent weight of the working electrode, □□the density of working electrode and A is exposed surface area of the working electrode in the test electrolytes. Corroded Specimens after corrosion testing were investigated at low and high magnifications using light and scanning electron microscopes.

Corrosion Test Results in simulated concrete pore solutions (Figure 1-6)

The electrochemical investigations of the steel substrates were carried out in simulated concrete pore solution. All the electrochemical experiments were performed using ACM instruments a Potentiostat/Galvanostat/FRA (model-Gill AC bistat) corrosion system at room temperature (20 ± 2 °C). A three electrode system was employed, where all specimens served as the working electrodes with an exposure area of 1 cm^2. The graphite and saturated calomel electrodes were utilized as the counter and reference electrodes, respectively. The open circuit potential (OCP) measurements were recorded for 1 hour to attain the stable and equilibrium potential. The potentiodynamic polarization experiments were performed from the cathodic region at −250 mV to the anodic region at +1500 mV with respect to the OCP, at a scan rate of 100 mV min^{-1}. The corrosion current density (i_{corr}) and corrosion potential (E_{corr}) were determined from the Tafel fitting and the corrosion rate was calculated in mm per year. All the electrochemical tests were repeated at least three times to confirm the reproducibility.

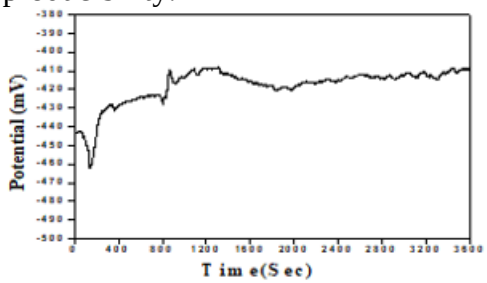

Figure 1: Open circuit potential of Steel-S simulated concrete pore solution.

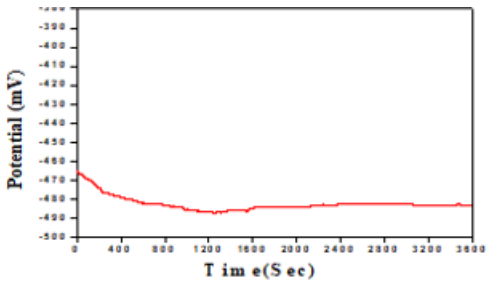

Figure 2: Open circuit potential of Steel-T in in simulated concrete pore solution.

OCP measures the free corrosion potential or equilibrium potential of the working electrode with respect to a reference electrode in an open circuit. The corrosion potential is moderated by the rate of oxidation and reduction due to the chemical reaction at the interface of the working electrode and electrolyte. We have, therefore, measured the OCP of the Steel-S and the result is compared with the OCP data of the Steel-T (figure 3). During the measurements, it was allowed one hour to attain the equilibrium potential and the fluctuation limit in the data within ± 10 mV is considered as a stable potential. The OCP measurements in SPS solution indicated that the stabilized potential of S sample is -410 mV_{SCE} and that of T sample is -482 mV_{SCE} as depicted in figure 3. Potential of S sample moves towards positive side where as T sample moves towards negative side. The higher value of the corrosion potential in case of Steel S than the Steel T indicates that the Steel S may be more protective against corrosion in SPS solution [6, 7]. However, OCP data is not sufficient to predict the

corrosion performance of the material as the measurement is carried out at the equilibrium condition. Therefore, the electrode kinetics on its surface may be different under dynamic condition. In view, we have performed the potentiodynamic polarization test to know about the corrosion current and corrosion rate of the both samples under dynamic condition.

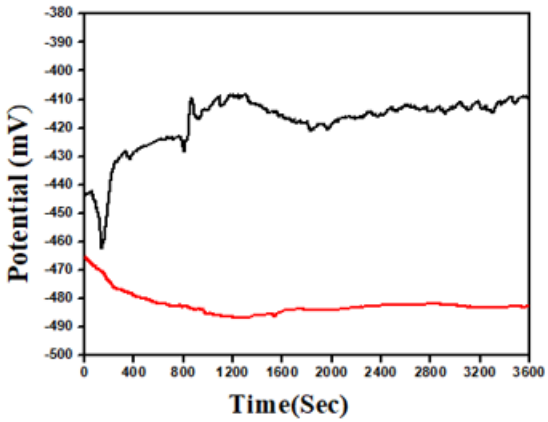

Figure 3: Open circuit potential of Steel-S versus Steel-T in simulated concrete pore solution.

The plot between current density and potential during potentiodynamic polarization test is known as Tafel plot which demonstrates the electrode kinetic behavior in electrolyte. The corrosion current density and corrosion rate are calculated from the potentiodynamic polarization measurement. In potentiodynamic polarization test, the potential is varied from cathodic region to anodic region with respect to the open circuit potential. Under controlled kinetic condition, the corrosion rate can be calculated from Tafel equation [8] that is

$$CR = k \times \frac{Icorr}{\rho \times A} \times Ew$$

Where k is the corrosion rate constant (3.27 x10^{-3} mm g/□A cm yr), Icorr is the corrosion current (□A), EW is the equivalent weight of the working electrode (27.92g), □□is the density of working electrode (7.87g/cm^3) and A is the exposed surface area of the working electrode (1 cm^2). The corrosion current (Icorr) of the respective Steel bar were calculated from intersect point by extrapolating the linear portion of the anodic and cathodic curves. The point of the intersection of the extrapolation on the X axis gives the value of Icorr for the respective bars. The corrosion current (Icorr) of the respective Steel bars were calculated from intersect point by extrapolating the linear portion of the anodic and cathodic curves. The point of the intersection of the extrapolation on the X-axis gives the value of Icorr of the respective substrates. Figure 6 displays the Tafel plot of Steel S as compared to the Steel T. The calculated values of corrosion current density (icorr) of the Steel S and Steel T are 0.0001127 mA/cm^2 and 0.0012389mA/cm^2 respectively. The Steel S sample shows less corrosion current and less corrosion rate than Steel T sample [9 -12].

Industrial Engineering Journal
ISSN: 0970-2555
Volume : 53, Issue 12, No.3, December : 2024

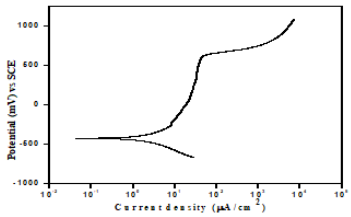

Figure 4: Potentiodynamic polarization curve of Steel-S in simulated concrete pore solution.

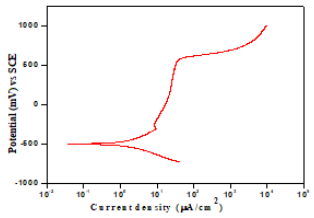

Figure 5: Potentiodynamic polarization curve of Steel-T in simulated concrete pore solution.

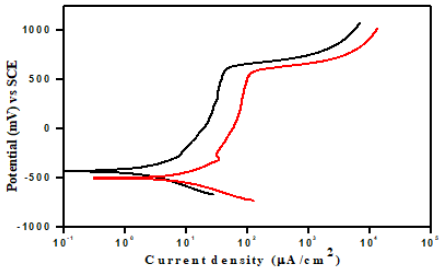

Figure 6: Potentiodynamic polarization curve of Steel-S versus Steel-T in simulated concrete pore solution.

Corrosion Test Results in simulated concrete pore solution with 3.5% NaCl (Figure 7-10)

The OCP measurements in SPS solution indicated that the stabilized potential of S sample is **-545 mV**$_{SCE}$ and that of T sample is **-405 mV**$_{SCE}$ as depicted in figure 7. Potential of S sample moves towards positive side where as T sample moves towards negative side. The higher value of the corrosion potential in case of Steel S than the Steel T indicates that the Steel S may be more protective against corrosion in SPS solution [8, 12, and 13]. The corrosion current (Icorr) of the respective Steel bars were calculated from intersect point by extrapolating the linear portion of the anodic and cathodic curves. The point of the intersection of the extrapolation on the X-axis gives the value of Icorr of the respective substrates. Figure 10 displays the Tafel plot of Steel S as compared to the Steel T. The calculated values of corrosion current density (icorr) of the Steel S and Steel T are **0.0010135** mA/cm^2 and **0.277587** mA/cm^2 respectively. The Steel S sample shows less corrosion current and less corrosion rate than Steel T sample [12-15].

Industrial Engineering Journal
ISSN: 0970-2555
Volume : 53, Issue 12, No.3, December : 2024

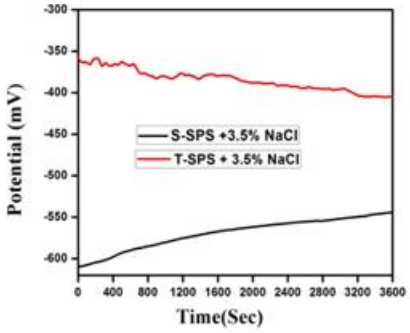

Figure 7: Open circuit potential of Steel-S versus Steel-T in simulated concrete pore solution with 3.5% NaCl.

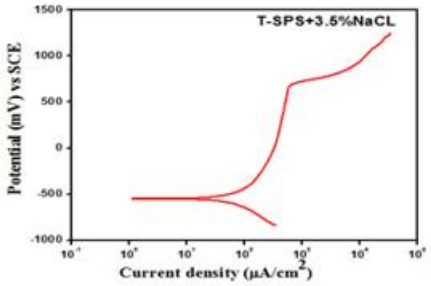

Figure 8: Potentiodynamic polarization curve of Steel-T in simulated concrete pore solution 3.5% NaCl.

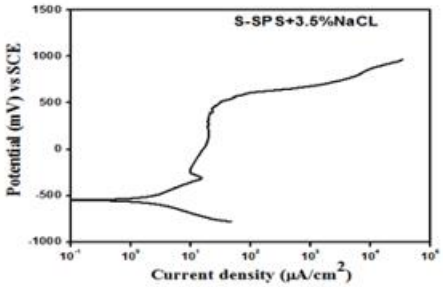

Figure 9: Potentiodynamic polarization curve of Steel-S in simulated concrete pore with solution with 3.5% NaCl.

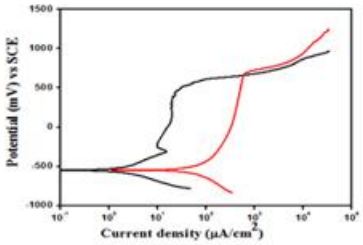

Figure 10: Potentiodynamic polarization curve of Steel-S versus Steel-T in simulated concrete pore solution with 3.5% NaCl.

Conclusions

It is observed from the experimental results that in presence of chloride ions, the corrosion rate of both the steel increases. However, both the steel corrodes in a significantly slower rate than that of the corresponding to conventional steel bars. From potentiodynamic results it is clearly indicated that corrosion of steel (sample-T-SPS) is more in comparison to steel (sample S-SPS) in simulated concrete pore solution and simulated concrete pore solution with addition of 3.5% NaCl. TMT steel bars containing sufficient amount of corrosion reducing alloying elements such as chromium, copper and nickel are more suitable for uses in the coastal as well as industrial areas where corrosion of steel bars is a great concern.

References

[1] Raharinaivo, M. Bouzanne, B. Malric, Influence of Concrete Aging on the Effectiveness of Monofluorophosphate for Mitigating the Corrosion of Embedded Steel, Proc Eurocorr '97, Trondheim, Norway, 22-25 Sept., (1997) 585.
[2] C. Alonso, C. Andrade, C. Argiz, B. Malric, Na2PO3F as inhibitor of corroding reinforcement in carbonated concrete, Cem Concr Res 26 (1996) 405- 416.

[3] K.K. Sagoe-Crentsil, F.P. Glasser, J.T.S. Irvine, Electrochemical characteristics of reinforced concrete corrosion as determined by impedance spectroscopy, Br Corros J 27 (1992) 113.
[4] R. Bhattacharya, G. Jha, S. Kundu, R. Shankar, N. Gope, Influence of cooling rate on the structure and formation of oxide scale in low carbon steel wire rods during hot rolling, Surf. Coat. Technol., 2006, 201, 526–532.
[5] R.J. Thibeau, C.W. Brown, R.H. Heidersbach, Raman spectra of possible corrosion products of iron, Appl. Spectrosc., 1978, 32, 532–535.
[6] R.J. Thibeau, C.W. Brown, R.H. Heidersbach, Raman spectra of possible corrosion products of iron, Appl. Spectrosc., 1978, 32, 532–535.
[7] J. Gui, T.M. Devine, Proc. of the 12th Int. Corrosion Congress, NACE International, Houstan, 1993, 2052.
[8] J. Dunnwald, A. Otto, An investigation of phase transitions in rust layers using Raman spectroscopy, Corros. Scie., 1989, 29, 1167 – 1176.
[9] T. Ohtsuka, K. Kubo, N. Sato, Raman spectroscopy of thin corrosion films on iron at 100 to 150 oC in air, Corrosion, 1986, 42, 476-481.
[10] T. Ohtsuka, Mater. Trans., Raman spectra of passive films of iron in neutral borate solution, Mater. Trans. JIM, 1996, 37, 67-69.
[11] M. Hanesch, Raman spectroscopy of iron oxides and (oxy)hydroxides at low laser power and possible applications in environmental magnetic studies, Geophys. J. Int., 2009, 177, 941-948.
[12] Y. N. Singhbabu, B. Sivakumar, J. K. Singh, H. Bapari, A. K. Pramanick and Ranjan K. Sahu Efficient anti-corrosive coating of cold-rolled steel in a seawater environment using an oil-based graphene oxide ink Nanoscale, 2015,7, 8035-8047
[13] R. A. Antunes, R. U. Ichikawa, L. G. Martinez, I. Costa, Characterization of corrosion products on carbon steel exposed to natural weathering and to accelerated corrosion tests, Interna. J. Corros., 2014, 1-9. http://dx.doi.org/10.1155/2014/419570.
[14] N. Boucherit, P. Delicher, S. Joiret, A. Hugot-Le Goff, Passivity of iron and iron alloys studied by voltammetry & Raman spectroscopy, Mater. Sci. Forum, 1989, 51, 44-45.
[15] D.C. Cook, S.J. Oh, R. Balasubramanian, M. Yamashita, The role of goethite in the formation of the protective corrosion on steels, Hyperfine Interactions, 1999, 122, 59-70.